X-RAY STRUCTURE AND PHASE TRANSFORMATIONS OF LiF CRYSTAL SURFACE UNDER GAMMA RADIATION

[1]Mussaeva Malika Anvarovna, [2]Elmurotova Dilnoza Bakhtiyorovna, [3]Raximova Yayra Maxmudovna, [4]Odilova Nelufar Jurayevna, [5]Tashmuxamedovna Sevara Nurullayevna

Senior Researcher Institute of Nuclear Physics RUz, PhD in Physics and Mathematics Science[1], Tashkent State Technical University named after Islam Karimov, PhD in Physics and Mathematics Science, assistant professor[2], TSTU, PhD in Physics and Mathematics Science, assistant[3], Karshi State University, assistant[4], TSTU, 1 course master[5]

mussaeva@inp.uz[1]

ABSTRACT

The obtained results on X-ray diffractometer of Empyrean pure crystals of LiF showed the presence of nanophase about 3% LiH and less than 1% Li_2O_2, responsible for the diffuse band at small angles and weak reflections near intense reflections (200) and (400) crystal matrix. And intensity irradiation of ^{60}Co gamma rays resulting grow phase LiH, LiO_2 and $(LiF)_2(B_2O_3)_3$, where at about annealing air 300 ^{0}C enhances oxide phases.

Key words: crystal, LiF, X-ray diffractometer, nanophase, gamma quantum, oxide phase.

INTRODUCTION

Alkali metal fluorides, which are ionic crystals with a cubic crystal structure, are finding ever wider practical application as optical materials for the vacuum ultraviolet range, due to equivalence webs, they are already widely used in radiobiology and medicine as thermo luminescent dosimeters of ionizing radiation, scintillation detectors of charged particles, active media for tunable color center lasers [1–3]. Due to the high quantum yield of luminescence, scintillation detectors for registration of neutrinos and thermal neutrons, thermo luminescent dosimeters of X- and gamma radiation, etc. have been developed on their basis. Colorless pure crystals of lithium fluoride were grown by the improved Kyropoulos method in a platinum dish in air from a reagent of high purity. For scintillator crystals, an impurity of copper oxide was added. Before measurements, the spent scintillator crystals were annealed at 350 ^{0}C for 1 hour to remove the radiation coloration. Thus, LiF can be used as a dosimeter with a limit of 10^7 R.

Earlier in work [4, 5], X-ray diffractometer (DRON-3M X-ray diffractometer) revealed gamma-induced Li nanocrystallites 8 nm in size after dry irradiation and LiOH 28 nm in length after wet irradiation.

PURPOSE OF THE STUDY

investigate possible changes in phase composition with nanoscale surface layers resulting from gamma irradiation crystals LiF.

MATERIAL AND METHODS

Objects – pure LiF crystals were chosen as a standard, from which plane-parallel plates 1–3 mm thick were chipped off, and samples of LiF cleaved from crystal with a volume of 2×2×7 cm^3.

Irradiation - samples were subjected to intense (1000 R/sec) of high (more than 10^8 R) ^{60}Co gamma-irradiation at a temperature below 270 K .

X-ray structural analysis. The structure parameters, the formation of dimensional defects and impurity phases, as well as mechanical stresses were investigated by wide-angle and small-angle X-ray structural analysis (XRA) on an improved Empyrean (Panalytical) instrument at 5-140 degrees, with a nickel filter and a high-aperture X-tube with Cu - cathode. Analysis of the obtained X-ray diffraction patterns makes it possible to determine the symmetry of the crystal structure, the crystallographic plane of the sample surface, and the general phase composition.

The collimation of an X-ray beam and the use of the small-angle scattering method make it possible to identify both amorphous regions and crystalline inclusions, and to determine their sizes on nanometer scale using the well-known Selyakov - Scherrer formula

$$L = 0{,}94 \cdot \lambda / \beta_{hkl} \cdot cos\Theta_{hkl}$$

Where L - is the grain size (nm), λ□□□is the wavelength of the radiation used (nm), θ - is the angle of reflection (radians), β - is the half-width of the corresponding reflection (rad).

Since the energy of X-ray radiation of 0.154 nm from copper tube is less than 50 keV, it penetrates into matter to depth of less than 100 μm, depending on its density and atomic number. Therefore, X-ray analysis is carried out in a thin near-surface layer, and not in the entire volume of the substance. Below in table 1 shows the technical characteristics of the Empyrean multifunctional X-ray diffractometer.

Table 1. Specifications multifunctional X-ray diffractometer Empyrean (Panalytical)

Configuration - Reflection – Transmission	Anode material Cu
Goniometer Theta/Theta radius mm [240.00, scan axis – Gonio]	K-alpha1 [Å] 1.54060 K-alpha2 [Å] 1.54443 K-A2/K-A1 ratio 0.50000
Minimum scan step 2Theta 0.0001	K-Beta [Å] 1.39225 cut by Ni filter
Start [2θ]-5.0039, end-139.9919, step [2θ] 0.0070, step time [s] 37.9950	X-radiation generator settings Current 40 mA, voltage 45 kV
Slit divergence [°] 0.4354	Sample thickness [mm] no more than 3
Distance from focus to slit [mm] 100.00	Sample length [mm] 10.00-30.00
Incident Beam Monochromator – No	Measurement temperature [^{0}C] 25.00±5
Measurement of X-spectra using the Data Collector software	Determination of the phase composition according to the PDF-2 database 2013
Stage with sample rotation in a horizontal plane with a minimum step of 0.1	X-ray processing (background level, peak identification, peak profile analysis) using the High Score program

RESULTS

Crystals LiF: Pure LiF crystals had cleaved (100) surface with an area of 2x2 and 1.5x3 cm; the base X-ray diffraction pattern and phase diagram are shown in Fig.1. Table 2 and 3 show the calculated structural characteristics.

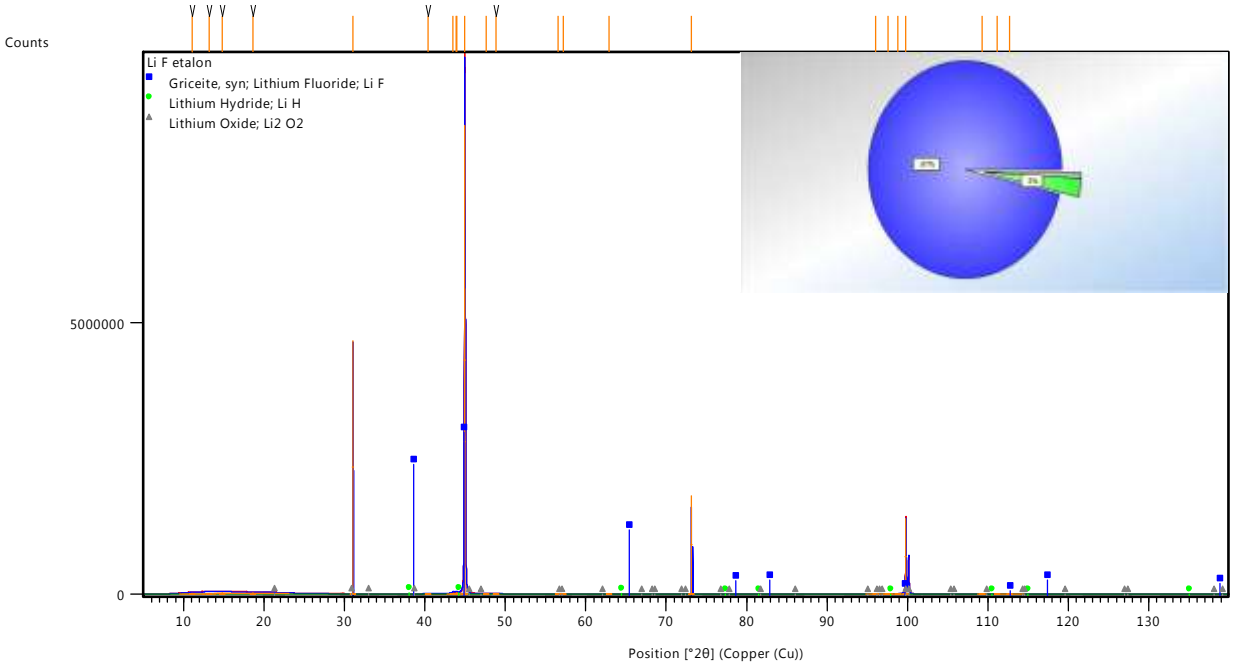

Fig. 1 X-diffraction spectrum and phase composition diagram of LiF crystal (reference)

Table 2. Structural characteristics of pure LiF crystal (reference), calculated using the High Score, FullProf program. The main reflections of the matrix and impurity phases are highlighted in color.

Peak position [2θ]	Peak height [cts]	Peak half-width left FWHM [2θ]	Distance between planes d [Å]	attitude of intensity [%]
11.0966	14391.23	3.1311	7.96711	0.17
13.1864	9640.25	1.7026	6.70880	0.11
14.8297	19864.54	1.9007	5.96886	0.23
18.6213	21232.04	8.9483	4.76119	0.25
31.0572	**4662212.00**	**0.0140**	**2.87727**	**54.10**
40.4220	882.72	0.7127	2.22966	0.01
43.5089	14202.76	0.2883	2.07835	0.16
43.8907	12651.64	2.2595	2.06115	0.15
43.9316	19277.18	0.3145	2.05933	0.22
44.9323	**8618183.00**	**0.0622**	**2.01576**	**100.00**
44.9705	**5621260.00**	**0.0409**	**2.01414**	**65.23**
47.5949	6981.66	0.5446	1.90902	0.08
48.8582	6717.70	0.5922	1.86257	0.08
73.1179	**1809238.00**	**0.0140**	**1.29321**	**20.99**
96.0244	788.73	2.5084	1.03634	0.01
97.5726	2215.96	1.2016	1.02398	0.03
98.7835	3213.81	2.3589	1.01465	0.04
99.8174	**1390514.00**	**0.0969**	**1.00690**	**16.13**
109.2958	825.18	1.1340	0.94444	0.01

111.1214	1067.18	0.4733	0.93401	0.01

Table 3. Phase composition of LiF crystal (reference), determined from the PDF-2 database

Reference code in the database	Score, point	Connection name	Offset angle [2θ]	Scale factor	Chem. formula
01-071-4663	10	Lithium fluoride (synthetic griceid)	-0.055	0.297	Li F
01-076-9249	6	Lithium hydride	-0.094	0.002	Li H
01-074-0115	4	Lithium oxide	-1.968	0.001	Li_2O_2

The surface cleaved along the (100) plane gives only two doublet ($K_{\alpha1}$ $K_{\alpha2}$) reflections: (200) at 44.93^0 and 44.97^0 with an intensity ratio of 100/65 and (400) at 99.82^0 and 100.2^0 with an intensity ratio of 15/7 (Table 2). The program identified the 97% crystal as a synthetic griceid, which is true. Since LiF is weakly hygroscopic, it was expected to detect lithium hydroxide, however, the program identified about 3% LiH and less than 1% Li_2O_2, because the samples were stored at low humidity. It should be noted insignificant (about 1^0) differences in the positions of reflections of the matrix crystal LiF and impurity nanocrystallites LiH, which ensures the coherence of their interphase boundaries. Very narrow and intense lines 31^0 and 73^0 and many weak reflections differ insignificantly from the basic spectrum of a macroscopic sample of Li_2O_2 with very low symmetry and can be attributed to one-dimensional nanocrystallites. The ratio of the scale coefficients of the main LiF (99) and impurity LiH-Li_2O_2 (1) phases and insignificant tensile stresses (negative displacement angle).

In fig. 2 shows an X-ray diffraction pattern and a phase diagram of LiF sample cleaved from crystal after gamma irradiation where, after which it acquired the nonlinear optical properties of a passive laser shutter and worked for more than 40 years [6–14].

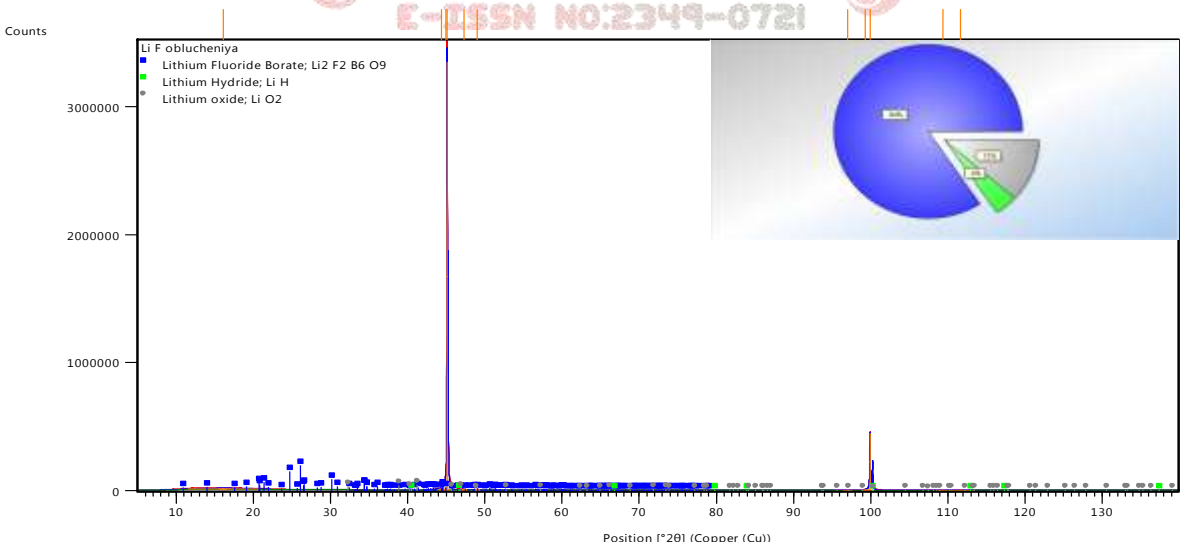

Fig. 2 X-diffraction spectrum and phase composition diagram of a pure LiF crystal irradiated in air at 320 K, ^{60}Co-gamma quanta at dose of 10^9 R

Table 4. Structural characteristics of pure LiF crystal irradiated in air at 320 K, ^{60}Co-gamma quanta at a dose of 10^9 R, calculated using the FullProf program

Peak position [2θ]	Peak height [cts]	Peak half width left FWHM [2θ]	Distance between planes d [Å]	attitude of intensity [%]
16.1406	8267.94	9.0314	5.48692	0.25
44.3961	16897.97	0.4638	2.03886	0.51
44.9081	22231.86	0.2249	2.01679	0.66
45.1194	**3345678.00**	**0.0639**	**2.00784**	**100.00**
47.2643	4504.59	0.5435	1.92160	0.13
49.0011	2130.51	0.8333	1.85748	0.06
96.9795	1406.27	1.0943	1.02866	0.04
99.2741	4791.88	0.9554	1.01095	0.14
99.9218	**445734.40**	**0.0900**	**1.00613**	**13.32**
109.3661	608.15	1.0725	0.94403	0.02

Table 5. The phase composition of a pure LiF crystal irradiated in air at 320 K ^{60}Co gamma quanta at dose of 10^9 R, determined from the PDF-2 database

Reference code in the database	Score, point	Connection name	mixing angle [2θ]	Scale factor	Chemical formula
01-080-9721	2	Lithium borate fluoride	-0.059	0.054	$Li_2 F_2 B_6 O_9$
01-076-9249	five	Lithium hydride	2.309	0.002	Li H
01-080-3472	2	Lithium oxide	3.415	0.011	$Li O_2$

Table 4. shows significant displacements of the reflections of the hydride and oxide phases of lithium in the direction of increasing angles, which indicates the compressive stresses of their lattices. Low scale coefficients indicate that these phases are located in a thin (less than micron) near-surface layer, under which the original bulk LiF crystal. If we estimate the volume of this impurity near-surface layer and the total number of even nuclei of Boron and Oxygen, then it should be equal to the number of gamma quanta absorbed by odd nuclei of Lithium and Fluorine, which in turn should be greater than or equal to Avogadro's number in order to provide a continuous volume of matter, detected and determined by the X-ray phase method (Table 5).

DISCUSSION

These results of the X-ray phase analysis of the composition of the near-surface layer of the gamma-irradiated sample confirmed the results of the study of the elemental composition by the energy dispersive method in a scanning electron microscope, where the peaks of the characteristic X-ray radiation of oxygen and boron were detected.

Possible photonuclear fusion reactions in a light LiF target with the highest atomic density:

$$_3Li^7 + {}_3Li^7 + \gamma\ (1.17\ МэВ) + \gamma\ (1.32\ МэВ) \rightarrow {}_4B^{11} + \alpha\ () + \ldots\ ;$$ and also F + F and Li + F

Vorobiev gives the results of registration of lithium decay products under the influence of neutrons from the reactor $_3Li^7 \rightarrow _2He^4 + _1T^3$ gas detectors [15, 16]. The formed gas pores with a size of 1–2 nm cause diffuse small-angle scattering of X-rays.

CONCLUSION

The use of a modern Empyrean X-ray diffractometer with spectra processing using the built-in High Score program and the international PDF-2 database made it possible to obtain the following results: In pure LiF crystals, nanophases of about 3% LiH and less than 1% Li_2O_2, responsible for diffuse band at small angles and weak reflections near the intense (200) and (400) reflections of the matrix crystal; After intense irradiation with ^{60}Co gamma quanta, the phases LiH, LiO_2 and $(LiF)_2(B_2O_3)_3$ grow, annealing in air at 300 ^0C also enhances the oxide phase.

The work was carried out under the program of fundamental research of the Institute of Nuclear Physics of the Academy of Sciences of the Republic of Uzbekistan (2021)

REFERENCES

1. T. Kurobori, T. Sakai, S. Aoshima // Phys. Status. Solidi A. 204, 699. (2007).
2. E.F. Martynovich, D.S. Glazunov, A.V. Kuznetsov, E.V. Pestriakov, A.V. Kirpichnikov, S.N. Bagayev. Optical sensors. // Opt. Soc. Am. (2011). Paper SWD6.
3. L.C. Courrol, R.E. Samad, L. Gomes, I.M. Ranieri, S.L. Baldochi, A.Z. Freitas, N.D.V. // Junior. Opt. Express. 12, 288 (2004).
4. Ibragimova E.M., Mussaeva M.A., Kalanov M.U., Mukhamedshina N.M. and Sandalov V.N. Lithium nanoparticles in lithium fluorite crystals // Journal of Phys. 2012. Conference Series 391. 012172. doi:10.1088/1742-6596/391/1/012172.
5. Mussaeva M.A., Ibragimova E.M., Kalanov M.U., Muminov M.I. Formation of nanodefects in LiF crystals at gamma-irradiation // Physics of the solid state. ISSN: 1063-7834. 2006. Vol 48. No 12. P. 2295–2299. https://doi.org/10.1134/S1063783406120092
6. Мартынович Е.Ф., Григоров В.А. Оптические свойства F2 - центров в монокристаллах фторида лития // ФТТ. 1980. Т.22. №5. Р. 1543 –1545.
7. Gellermann W., Muller A., Wandt D. Formation, optical properties, and laser operation of F-2 centers in LiF // Journal of Applied Physics. 1987. 61. 1297. https://doi.org/ 10.1063/1. 338107
8. W. Gellermann. Color center lasers //J. Phys. Chem. Solids. 1991. Vol. 52. Issue 1. Pages 249–297. https://doi.org/10.1016/0022-3697(91)90068-B.
9. Т.Т. Басиев, А.Н. Кравец, А.В. Федин. Модуляция добротности технологического ИАГ: Nd-лазера кристаллами LiF:F2 - при импульсно-периодической накачке // Квантовая электроника. 1993. Т.20. № 6. С. 594–596.
10. T.T. Basiev, A. Lucianetti, R. Weber, W.Hodel, H.P. Weber, A.G. Papashvili, V.A. Konyushkin // Appl. Opt. 1999. 38. 1777.
11. T.T. Basiev, S.V. Vassiliev, V.A. Konjushkin, V.P. Gapontsev. Pulsed and cw laser oscillations in LiF:F-2 color center crystal under laser diode pumping // Opt. Lett. 2006. Vol. 31. Lssue 14. 2154–2156. https://doi.org/10.1364/OL.31.002154.
12. Л.А. Лисицына, В.М. Лисицын. Состав нанодефектов в активированных кристаллах фторида лития // ФТТ. 2013. Т. 55. вып. 11. С. 2183–2189.

13. R.A. Bigelow NUCRAD. Chapter 5. Radiation interactions in matter. 1992. P.98–116.
14. Okuda, Kazuo Makishima, Mitsuteru Sato, Yousuke Sato, Toshio Nakano, Daigo Umemoto, Harufumi Tsuchiya / Photonuclear reactions triggered by lightning discharge // Nature.2017. V.551. P.481–484. doi:10.1038/nature24630.
15. М. Борн. Динамическая теория кристаллических решеток. Перевод с английского В. И. Когана. Под ред. И. М. Лифшица. – М.: Иностранная литература. 1958. 488 с.
16. А.А. Воробьев Механические и тепловые свойства щелочно-галоидных кристаллов. –Москва.: Высшая школа. 1968. 272 с.